

# The influence of lateral heel flare of running shoes on pronation and impact forces

BENNO M. NIGG and M. MORLOCK

*Human Performance Laboratory,  
University of Calgary,  
Calgary, Alberta, CANADA T2N 1N4*

## ABSTRACT

NIGG, B. M. and M. MORLOCK. The influence of lateral heel flare of running shoes on pronation and impact forces. *Med. Sci. Sports Exerc.*, Vol. 19, No. 3, pp. 294-302, 1987. The purpose of this investigation was to study the influence of the flare at the lateral side of the heel of running shoes on: (a) initial and total pronation; (b) impact forces in heel-toe running; and (c) to explain the results with a mechanical model. The experimental part of the study was performed by using 14 male runners. Their running movement (4 m/s) was quantified by using a force platform and high-speed film (100 frames·s<sup>-1</sup>). Three shoes were used, identical except in their lateral heel flare, one shoe with a conventional flare of 16°, a second shoe with no flare, and a third shoe with a rounded heel (negative flare). The experimental results indicate that (for the used set of shoes);

- 1) increasing heel flare increases the amount of initial pronation;
- 2) changes in heel flare do not affect the magnitude of the total pronation; and
- 3) changes in heel flare do not alter the magnitude of the impact force peaks.

Since shoes with rounded lateral heels do reduce initial pronation, it is speculated that this construction could be used to prevent anterior medial compartment syndrome at the tibia of runners. It was concluded that more research is needed to specify whether the reported result is representative for various shoe types or is shoe specific.

PRONATION, IMPACT FORCES, RUNNING, LOAD,  
BIOMECHANICS, KINEMATICS, KINETICS

Research about running shoes in the last 10 yr yielded three general conclusions. (a) Running shoes should be built to reduce impact forces in the first 30 to 50 ms of ground contact (3, 5, 10, 11, 17, 19), since these impact forces are assumed to be associated with injuries such as fatigue fractures, tendinitis, and cartilage damage (20, 22, 28). (b) Running shoes should be built to provide medio-lateral stability, sometimes referred to as rearfoot control (2, 4, 7, 17, 24), since medio-lateral instability is assumed to be connected with over-use injuries such as anterior medial compartment syndrome or ilio-tibial band syndrome (8, 13, 21, 22, 27). (c) Running shoes should be built to provide guidance to avoid over-supination of the foot during the take-off phase (18, 19, 24), since over-supination at take-off is

speculated to be connected with Achilles tendon problems (19, 23).

These three main conclusions are widely accepted. However, there is considerable discussion on which strategies to choose to reach the goal described in these three conclusions. One important aspect is the control of medio-lateral stability. Various constructional aids such as heel stabilizers, wedges, double density soles, various heel flares, and heel caps are offered in an attempt to reduce pronation and to increase "rearfoot stability."

However, instead of discussing various strategies to reduce excessive pronation, one can discuss possibilities to avoid it. One strategy is based on the assumption that a wide heel on the lateral side is one possible reason for excessive pronation in heel-toe running (6, 19). If this assumption is correct, the logical consequence is to construct the heel of the running shoe so that the moment of rotation responsible for pronation is reduced. The shoe construction that fulfills these requirements is a construction with a rounded lateral heel.

The purpose of this paper is to study the influence of sole geometry (flare at the lateral side of the heel of running shoes) on: (a) initial and total pronation; (b) impact forces in heel-toe running; and (c) to explain the results with a mechanical model.

## MATERIALS AND METHODS

The subtalar and ankle joint perform a complex motion during ground contact in running (7). Pronation of these joints consists of simultaneous eversion, abduction, and dorsiflexion. Supination of these joints involves inversion, adduction, and plantar flexion (12). Rearfoot movement during ground contact was quantified using markers on the heel of the shoe and at the posterior aspect of the lower leg (1, 4, 6, 7). Marker A was located 15 cm above marker B in the center of the leg (rear view) in the standing position (barefoot). Marker B was located on the Achilles tendon just above the heel cap of the shoe. Marker C was located on the

upper part of the heel cap. Marker D was located in the center of the shoe sole (posterior view). Markers C and D were located so that the line between C and D and the horizontal form an angle of  $90^\circ$  in the unloaded shoe. The projection of these markers in a plane perpendicular to the running direction was used to define the rearfoot angle,  $\gamma$ , between the markers on the heel and the horizontal on the medial side and the Achilles tendon angle,  $\beta$ , between the markers on the lower leg and the markers on the heel on the medial side (Fig. 1). The method (16) describes the motion of the shoe with its rearfoot angle,  $\gamma$ , and the motion in the joints (subtalar and ankle joint) with its Achilles tendon angle,  $\beta$ . Because of the two-dimensional limitation of this method, real rotation around ankle and/or subtalar joint cannot be determined.

The movement of the leg was also quantified using markers on the lateral aspect of the leg (Fig. 1), providing the knee angle,  $\epsilon$ , measured at the posterior side and the sole angle,  $\delta$ , measured between ground and shoe (positive for heel landing). The markers were located as follows: marker E was located at the mid-sole of the forefoot at the head of the fifth metatarsal. Marker F was located at the mid-sole of the heel underneath the calcaneus. Marker G was located at the lateral malleolus. Marker H was located at the head of the fibula. Marker I was located above the knee joint (tibio-femoral joint on a middle line for lateral view in the standing position), and marker K was located in the similar way as marker I, but two-thirds of the distance between the tibio-femoral joint and the hip joint.

It is obvious that markers on the skin of the subject or on the outside of the shoe do not provide an accurate location of skeletal landmarks. Absolute values of these angles are therefore affected with possible systematic errors due to relative skin movement. However, it has been shown that relative values (changes in these angles) are less sensitive to systematic errors (18) than absolute

values. In this analysis, therefore, main emphasis will be given to angular changes during movement.

External impact forces were determined by measuring ground reaction forces during the first 50 ms. A Kistler force platform was properly mounted in the runway providing four vertical, two medio-lateral, and two antero-posterior force outputs. These outputs were used in a PDP-11/44 computer system to calculate the components of the resultant ground reaction forces. Note that external impact forces are not identical with the internal impact forces in the ankle or knee joint. External impact forces which may be the cause of overloading of internal structures during the impact phase depend on: (a) initial conditions such as velocity of touch down of the heel, position of foot and lower leg and angle of the knee at first contact; and (b) boundary conditions such as shoe sole material and surface.

The experimental part of the study was conducted with 14 male runners with a mean mass of 69.8 kg (SD = 5.3 kg). All of them were runners with a minimal weekly distance of 15 km. Informed consent was obtained from all subjects who volunteered to participate. Three pairs of running shoes (Adidas ZX 600, size 9) were used in the study. They were identical in construction (Shore 42 to 43 for the harder and Shore 36 to 37 for the softer part of the mid-sole), except in the geometrical shape of the lateral posterior part of the shoe sole. Shoe A had a conventional heel with a flare of  $16^\circ$  at the lateral side. Shoe B had no flare, and shoe C had the lateral heel part rounded (radius about 3 to 4 cm), providing a negative flare with a non-constant value (Fig. 2). The subjects had to run over a force platform (Kistler, Type Z4852/C) with a natural frequency of at least 250 Hz on each channel and a sampling rate of 1,020 Hz for each channel. The runway was about 16 m long with the force platform located in the middle of the runway. Each subject performed as many practice runs as needed in order to land consistently on the force platform with the right foot. Each subject performed one trial per shoe. The running velocity was  $4 \pm 0.2$  m/s and was controlled by photocells which were mounted 1 m from the center of the force platform in both directions at hip height. Trials where the running

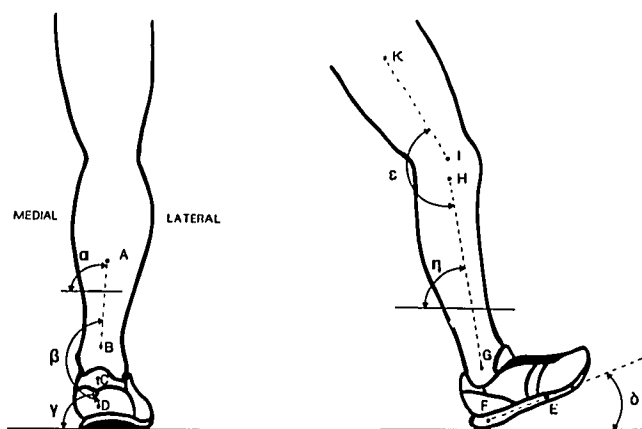


Figure 1—Illustration of the variables and symbols used in film analysis for running shoe research.  $\beta$  = Achilles tendon angle,  $\gamma$  = rearfoot angle,  $\delta$  = sole angle,  $\epsilon$  = knee angle.

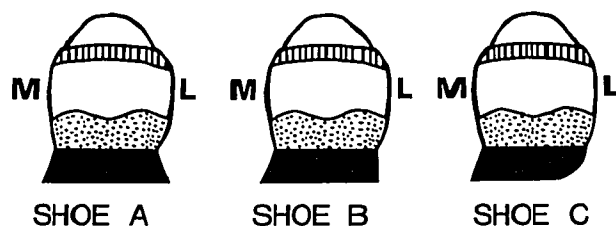


Figure 2—Schematic illustration of the different flare values on the lateral (L) side of the running shoes used in this study. Shoe A has a flare of  $16^\circ$ , shoe B has no flare, and shoe C has a negative flare. M = medial.

velocity was outside the prescribed range or where the foot was outside the force platform area were discarded. Simultaneously, film measurements were taken from posterior and lateral views with a film frequency of 100 frames  $\cdot$  s $^{-1}$ .

The variables discussed in this context can be categorized in three groups:

1) Variables describing pronation. They include:

$\Delta\beta_{10}$  = initial joint pronation; change of the Achilles tendon angle in the first tenth of foot contact time

$\Delta\gamma_{10}$  = initial shoe pronation; change of the rearfoot angle in the first tenth of foot contact time

$\dot{\beta}_{10}$  = initial joint pronation velocity; mean angular velocity of the Achilles tendon angle in the first tenth of foot contact time

$\dot{\gamma}_{10}$  = initial shoe pronation velocity; mean angular velocity of the rearfoot angle in the first tenth of foot contact time

$\Delta\beta_{pro}$  = total joint pronation; total change of the Achilles tendon angle from first contact to its maximal value

$\Delta\gamma_{pro}$  = total shoe pronation; total change of the rearfoot angle from first contact to its maximum value.

2) Variables describing initial conditions. They include:

$\beta_0$  = initial Achilles tendon angle (all initial variables are determined from the last film frame before ground contact)

$\gamma_0$  = initial rearfoot angle.

$\delta_0$  = initial sole angle; angle between the horizontal and the shoe sole immediately before ground contact (lateral view)

$\epsilon_0$  = initial knee angle. Angle between the lower leg and the thigh immediately before ground contact (lateral view)

$v_{oz}$  = vertical touch down velocity of heel measured with point F in Figure 1

$v_{oy}$  = anterior-posterior touch down velocity of heel.

3) Variables describing ground reaction forces. They include:

$F_{zi}$  = vertical impact force peak; relative maximum of the vertical ground reaction force in the first 50 ms

$t_{zi}$  = time occurrence of impact force peak

$G_{zi}$  = maximum vertical loading rate; maximum time derivative in vertical direction of  $F_z(t)$  before reaching the impact peak.

The film and force variables are defined and discussed in detail elsewhere (16). Statistical comparison of the

results of shoes A and C was done using a one-way analysis of variance with a multiple range test (Tukey-B procedure) and a 0.05 level of confidence.

## RESULTS

The results are reported and discussed from three viewpoints: (a) variables describing pronation; (b) variables describing initial conditions; and (c) variables describing forces. A summary of the results is presented in Appendix 1.

**(a) Variables describing pronation.** The influence of different lateral heel flare constructions on initial pronation is illustrated in Figure 3. The mean values decreased from shoe A to shoe B to shoe C which means from positive to negative flare for both the initial joint pronation and the initial shoe pronation. A comparison of the results for shoe A with the results for shoe C shows a reduction of about 40% for the initial joint pronation  $\Delta\beta_{10}$  and a reduction of about 45% ( $P < 0.05$ ) for the initial shoe pronation  $\Delta\gamma_{10}$ . The reduction is similar for the mean initial pronation velocity, since this variable is calculated by dividing the initial pronation by 10% of the contact time. The contact time, however, did not change significantly for the three shoe types.

The influence of lateral heel flare designs on total pronation is illustrated in Figure 4. The mean values are between 14.1° and 15.1° for the total joint pronation and 11.4° and 12.7° for the total shoe pronation and do not differ significantly for the three shoe types used. A change of the lateral heel flare influences therefore the initial pronation and the initial pronation velocity (angular velocity) for joint and shoe but does not influence the total pronation for both joint and shoe for the shoes and subjects used in this experiment.

### INITIAL PRONATION

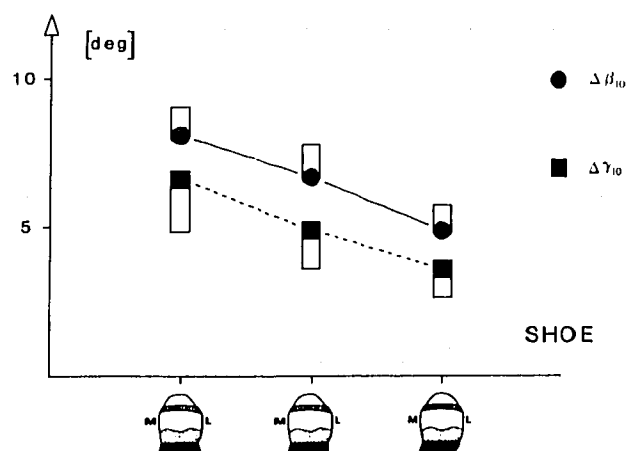


Figure 3—Influence of different lateral (L) heel flare constructions on initial pronation during the first tenth of ground contact time described by the change of the Achilles tendon angle,  $\beta$ , and the rear foot angle,  $\gamma$ , (mean and SE). M = medial.

## TOTAL PRONATION

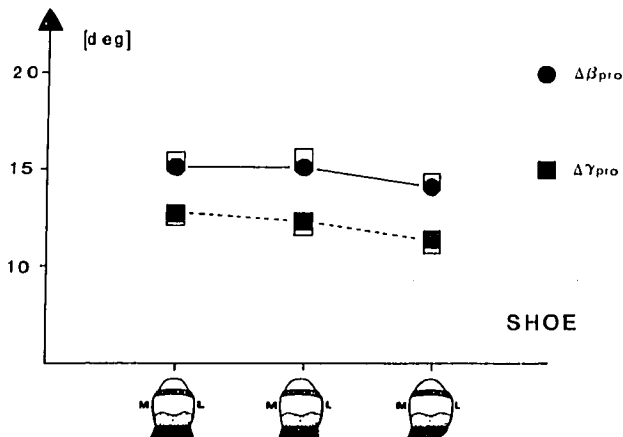


Figure 4—Influence of different lateral (L) heel flare construction on total pronation described by the change of the Achilles tendon angle,  $\beta$ , and the rear foot angle,  $\gamma$ , (mean and SE). M = medial.

(b) **Variables describing initial conditions.** The influence of lateral heel flare designs on variables describing initial conditions is illustrated in Figure 5. The initial Achilles tendon angle,  $\beta_o$ , and the initial sole angle,  $\delta_o$ , do not show a significant change. However, the initial rearfoot angle decreases as the flare angle decreases by  $3^\circ$  ( $P < 0.05$ ). This change indicates a flatter landing of the shoe sole for shoe C compared to shoe A. The touch-down velocity increases from 0.9 to 1.06 m/s (an increase of 18%), as the flare angle decreases from shoe A to shoe C. However, the change is not significant on the 5% level due to large inter-individual variation. Additionally, the knee angle,  $\epsilon_o$ , measured from the lateral view does not change significantly due to different lateral heel flares. A change of the lateral heel flare influences therefore the sole position of the shoe for the shoes and subjects used in this experiment.

(c) **Variables describing force.** The influence of lateral heel flare on impact force variables is illustrated in Figure 6. The mean values of the vertical impact force peaks,  $F_{zi}$ , and the maximal loading rate,  $G_{zi} = (dF_z/dt)_{max}$ , do not change significantly due to the different heel flare. However, the time of occurrence of the impact peak changes from 37.6 ms for shoe A with the conventional positive flare to 29.1 ms (a decrease of 29%) for shoe C with the rounded heel (negative flare). A change of lateral heel flare influences therefore the time of occurrence of the impact force peak but not the magnitude of impact force peak and maximum loading rate for the shoes and subjects used in this experiment.

## DISCUSSION

(a) **Variables describing pronation.** The reduction of initial pronation and initial pronation velocity as the flare angle decreases was expected. It is connected with

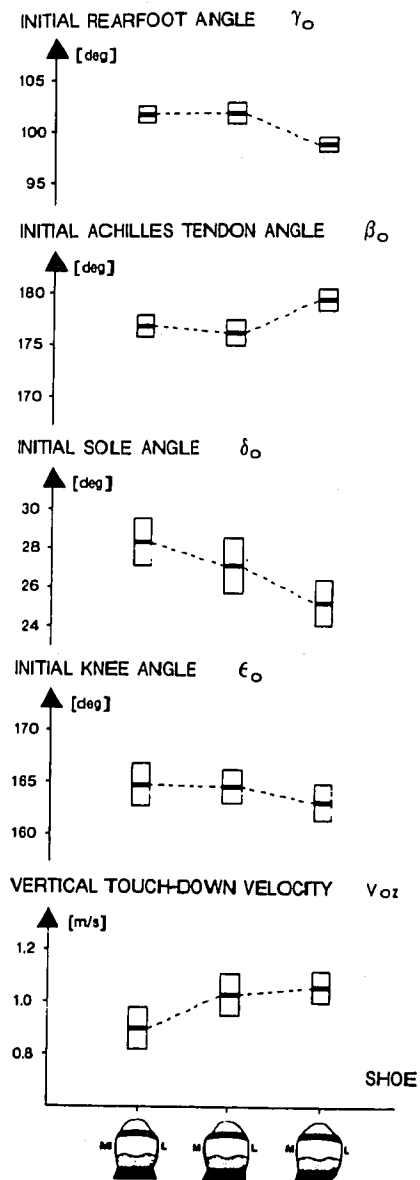


Figure 5—Influence of different lateral (L) heel flare construction on initial conditions describing position of foot ( $\gamma_o$  and  $\delta_o$ ) and leg ( $\beta_o$  and  $\epsilon_o$ ) and touch-down velocity ( $V_{oz}$  (mean and SE). M = medial.

a change in lever arm as illustrated in Figure 7 for one subject 14 ms after first ground contact. The external resultant force acting on the shoe with the rounded heel has a smaller lever arm with respect to the subtalar joint axis and causes therefore less initial pronation and a smaller initial pronation velocity. This explanation is supported by a general discussion of the influence of lever arm on initial pronation for running with a conventional running shoe with positive flare compared to barefoot running (25). The model of reduced initial pronation in this experiment is also supported by results of another experiment where shoes with different mid-sole hardnesses are compared (19). For the softer shoe, the material at the lateral side of the heel is more compressed than for the harder material, and the lever arm of the acting resultant force with respect to the

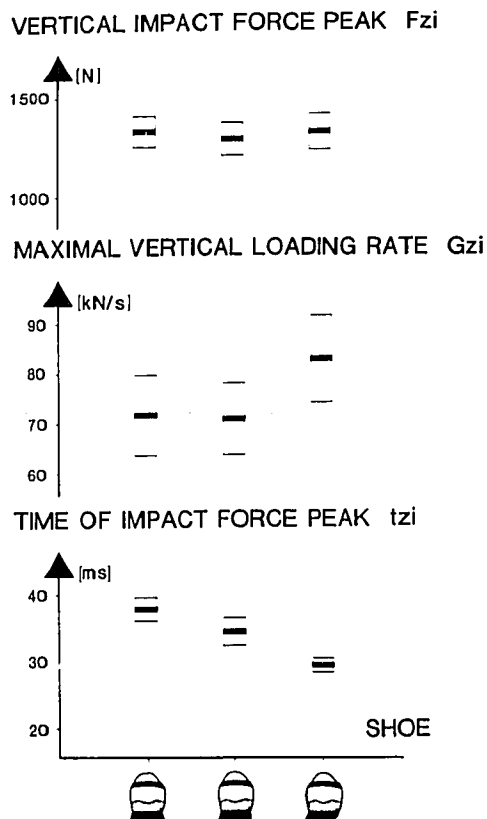


Figure 6—Influence of different lateral heel flare construction on vertical impact force peak,  $F_{zi}$ , its time of occurrence,  $t_{zi}$ , and the maximum loading rate,  $G_{zi}$ .

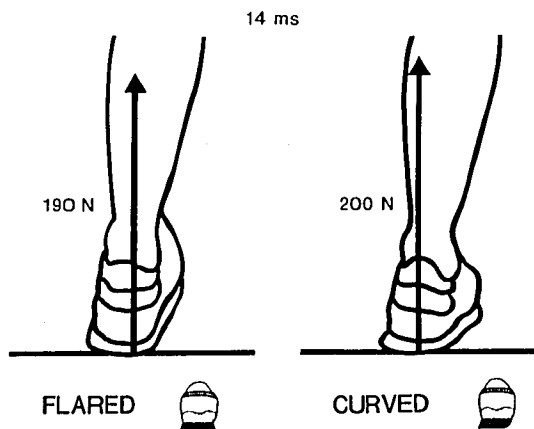


Figure 7—Illustration of the external ground reaction force for one subject running with a shoe with a round heel (*right*) and a shoe with a flared heel (*left*) for a running speed of 4 m/s.

subtalar joint axis is reduced as illustrated in Figure 8 for one subject running with a shoe with a soft (shore 25) and a hard (shore 45) mid-sole. The softer mid-sole results therefore in a decreased initial pronation. In all three examples (our experiment, the theoretical discussion, and the experiment with the different sole hardnesses), the mechanical consideration and experimental results for initial pronation are in agreement.

The result that total pronation is not influenced by

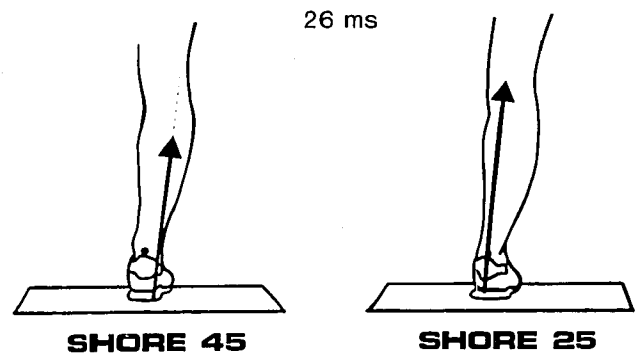


Figure 8—Illustration of the resultant external ground reaction force for one subject running with a shoe with a soft (shore 25) and a hard (shore 45) mid-sole 26 ms after first ground contact ( $v = 4$  m/s).

the geometrical construction of the lateral heel flare in our experiment may seem surprising. It certainly was not expected, based on results of an earlier experiment (15, 19) which compared total pronation for two shoes, a shoe P with a nylon upper, a (conventional) positive heel flare, and a relatively weak medial mid-sole construction and a shoe Q with a leather upper, a negative heel flare, and a relatively stable mid-sole construction. This earlier experiment showed for two subjects with extensive total pronation a reduction of total pronation from 21° and 31° for shoe P to 12° for shoe Q. A possible explanation of the results of the current (shoes A, B, and C) and the previous (shoes P and Q) experiment may be found in: (a) the upper and mid-sole construction; and (b) the amount of pronation. The fact that shoe P had less medial support than shoes Q, A, B, and C may be the reason for the excessive pronation. In addition, the current experiment with shoes A, B, and C did not include subjects with excessive pronation of more than 25°. These considerations suggest that total pronation is connected with the mid-sole hardness on the medial side beneath the arch or generally with the medial stability of a shoe.

If these assumptions and conclusions are correct, one would speculate that

- 1) the geometrical construction of the lateral heel flare has little influence on total pronation of the running shoe if the medial side of the shoe is stable and firm and that
- 2) the geometrical construction of the lateral heel flare may have influence on total pronation if the running shoe at the medial side provides little support.

However, these speculations have yet to be supported by further experimental and/or theoretical evidence before they can be accepted.

Frederick and co-workers (11) and Clarke and co-workers (6) studied the influence of lateral heel flare (0°, 15°, and 30°) on maximum pronation for three

different mid-sole hardnesses. They found for hard mid-soles (shore 45 for mid-sole material) no difference in maximum pronation. For medium (shore 35) and soft (shore 25) mid-sole hardnesses, they found maximum pronation to increase with decreasing flare. Their results for the hard mid-soles are similar to the results of our study. However, their results for medium and soft mid-soles disagree with our results and are opposite to the speculations made in this paper. The obvious discrepancy may be: (a) due to different shoe types; (b) due to the fact that they studied treadmill running while this study analyzes over-ground running; (c) due to the fact that their maximum pronation is an angle with respect to a vertical line while our total pronation is an angle difference (maximum minus initial value); or (d) due to the fact that they studied flare changes in the positive range while we studied changes in a range between positive and negative.

**(b) Variables describing initial conditions and external forces.** The two initial conditions that changed from the conventional shoe A to the rounded heel shoe C were the vertical touch-down velocity and the rearfoot angle. The increase of the mean touch-down velocity (18%) is assumed to affect the magnitude of the impact force peaks. In addition, the decrease in the rearfoot angle,  $\gamma$ , increases the stiffness of the shoe sole and would therefore increase the impact force peak likewise. One would therefore expect the impact force peaks to increase for the rounded heel shoe C compared to the conventional shoe A. The order of magnitude of this expected increase is about 20%. However, the experimental results do not show such an increase and contradict expectations and "common sense." A simple spring mass model for ideal heel landing, as suggested by Denoth (9), can be used to explain the results of this experiment for the impact force peaks:

$$F_{zi} = v \cdot \sqrt{f} \cdot \sqrt{m^*} \quad [1]$$

where

- $v$  = touch-down velocity (vertical)
- $f$  = spring constant of the shoe-heel system
- $m^*$  = effective mass (mass primarily involved in the deceleration process) (9)
- $F_{zi}$  = maximum vertical impact force.

The relative change in impact peak can be described as:

$$\Delta F:F_0 = [v_0 \cdot \sqrt{f_0} \cdot \sqrt{m_0^*} - v_1 \cdot \sqrt{f_1} \cdot \sqrt{m_1^*}] / [v_0 \cdot \sqrt{f_0} \cdot \sqrt{m_0^*}] \quad [2]$$

This change depends on: (a) the change of the vertical touch-down velocity which can be determined from the experimental results; (b) the change in the spring stiffness of the heel-shoe system which can be determined as described in Appendix 2; and (c) the change in the effective mass. The effective mass depends on the knee

angle at touch down (9, 15). However, the knee angle at touch down does not show a significant difference between shoe A and shoe C ( $166.0^\circ$  compared to  $164.3^\circ$ ). Furthermore, the "effective mass depends heavily on the time characteristics of the impact force. It is increasing with decreasing frequency of the impact force" (9). An experimental example for this theoretical statement (the influence of the occurrence in time,  $t_{zi}$ , on the vertical impact force peak) is illustrated in Figure 9 for one subject. The effective mass was experimentally determined by using its definition (9):

$$m^* = \frac{F_z}{a_t + g} \quad [3]$$

where

- $F_z$  = vertical impact force
- $a_t$  = acceleration at the tibia
- $g$  = acceleration due to gravity.

The values obtained in this experiment with one subject are used in the following to estimate the order of magnitude of impact force peaks expected in this experiment. The time of occurrence,  $t_{zi}$ , of the impact force peak changed from 37.6 ms for the conventional shoe A with positive flare to 29.1 ms for shoes with the rounded heel. This changes the effective masses for these two cases from about 73 to 58 kg using the values of the least-squares fit curve through the experimental results.

Substituting all the discussed effects in equation 2, the relative change of external impact forces in this experiment is predicted to be small (5.3%). In other words, the experimental result of the non-changing impact force peaks can be understood by using a simple effective mass-spring model in which the experimental

EFFECTIVE MASS  $m^*$

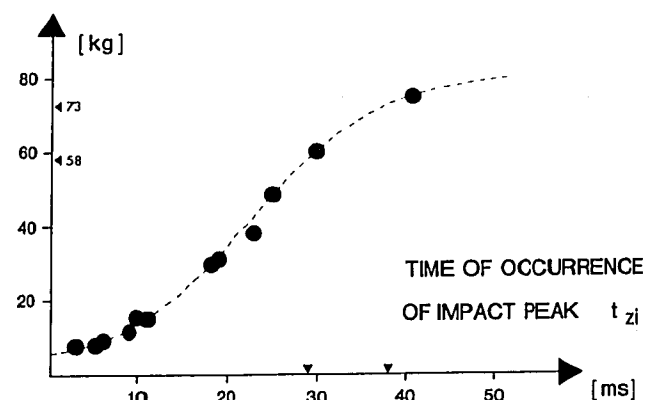


Figure 9—Experimental determination of the effective mass as a function of the time of occurrence,  $t_{zi}$ , of the impact force peak measured with the force platform and an accelerometer mounted at the anterior part of the ankle joint of one subject for running barefoot on various surfaces (from steel to very soft).

results for initial and boundary conditions as well as the first part of the movement are included. However, these calculations and discussions explain only that it can be understood in a mechanical sense that the impact force peaks do not change. They do not explain why this strategy is chosen by the subjects or why, for instance, the touch-down velocity of the heel increases.

The result, that the external vertical impact force peak remains constant, is consistent with previous experiments where impact force peaks were assessed for running with different mid-sole hardnesses and running with additional weights at the foot, tibia, and hip (19). In both experiments, the mean vertical impact force peaks did not change. The result of constant impact force peak is now, for the third time, repeated. The meaning of the result is not yet evident. However, it could be that the solution of this question provides a general answer to the question of what rules govern the landing strategies in heel-toe running.

**(c) Relevance of the findings.** Excessive initial pronation and initial pronation velocity are assumed to be connected with over-loading of the anterior part of the tibia ("shin splint") and the anterior and medial part of the tibio-femoral joint. Excessive total pronation is assumed to be connected with over-loading of the medial structures at the ankle joint (posterior tibial tendinitis and plantar fasciitis) and due to rotation of the tibia excessive pronation is assumed to be connected with patellar tendinitis and ilio-tibial band syndrome. The findings and conclusions from this study are expected to have an influence on prevention and/or treatment of over-loading injuries due to excessive pronation.

A running shoe with a rounded heel at the lateral posterior side of the shoe sole can therefore be used:

- 1) to produce running with small initial pronation in all shoes, and
- 2) to limit the total pronation in shoes with little support at the medial side of the shoe.

In both cases, loading may be reduced if a shoe heel is changed from positive flare to round heel or over-loading may be prevented if a round heel is used in a

non-pathological situation. The difference of this approach compared with the conventional methods (e.g., heel stabilizers) lies in the fact that *pronation is avoided* instead of reduced.

The fact that sport and especially knee injuries increase in importance and relative frequency (4, 26) indicates that ligaments, tendons, and cartilage are loaded with forces close or above the critical limits (14, 29). The proposed and described conservative approach of changing the shape of the lateral and posterior heels (rounded heels) is assumed to reduce the loading in these structures and to reduce therefore the frequency of injuries caused by excessive pronation.

## SUMMARY

The experimental analysis of the influence of sole geometry (flare) at the lateral and posterior sides of the heel of running shoes on initial and total pronation in heel-toe running can be summarized as follows. (a) Initial pronation and initial pronation velocity are significantly influenced by the sole flare on the lateral heel. Negative flare has less initial pronation than positive flare. (b) Total pronation was not influenced in this experiment by changed heel flare. It is speculated that changes in lateral heel flare have an influence on total pronation if the running shoe at the medial side provides little support. Conversely, one might speculate that total pronation is most greatly influenced by the construction of the medial aspect of the shoe (i.e., sole and upper). (c) Impact force peaks did not change as a consequence of changed lateral heel flare in this experiment.

The use of a rounded heel is therefore assumed to have a positive influence in reducing and/or preventing running injuries.

This study was supported by grants from the Natural Sciences and Engineering Research Council of Canada, Alberta Heritage Foundation for Medical Research, and Adidas (Sport Shoe Company).

The outstanding contributions of Veronica Fisher, Byron Tory, and Bob Glover in the data collection and analysis are appreciated.

Address for correspondence: Benno M. Nigg, Human Performance Laboratory, University of Calgary, 2500 University Drive, N.W., Calgary, Alberta, Canada T2N 1N4.

## REFERENCES

1. BATES, B. T., L. R. OSTERNIG, and B. MASON. Lower extremity function during the support phase of running. In: *Biomechanics VI-A*, E. Asmussen and K. Jorgensen (Eds.). Baltimore, MD: University Park Press, 1978, pp. 31-39.
2. BATES, B. J., L. R. OSTERNIG, B. R. MASON, and S. L. JAMES. Functional variability of the lower extremity during the support phase of running. *Med. Sci. Sports* 11:328-331, 1979.
3. CAVANAGH, P. R. Testing procedure. *Runner's World* 10:70-80, 1979.
4. CAVANAGH, P. R. *The Running Shoe Book*. Mountain View, CA: Anderson World, Inc., 1980, pp. 145-148.
5. CAVANAGH, P. R. and M. A. LAFORTUNE. Ground reaction forces in distance running. *J. Biomech.* 13:397-406, 1980.
6. CLARKE, T. E., E. C. FREDERICK, and C. L. HAMILL. The effects of shoe design parameters on rearfoot control in running. *Med. Sci. Sports* 15:376-381, 1983.
7. CLARKE, T. E., E. C. FREDERICK, and C. L. HAMILL. The study of rear foot movement in running. In: *Sport Shoes and Playing Surfaces*, E. C. Frederick (Ed.). Champaign, IL: Human Kinetics Publishers, 1984, pp. 166-189.
8. CLEMENTS, D. B., J. E. TAUNTON, G. W. SMART, and K. L. MCNICOL. A survey of overuse running injuries. *Physician Sports Med.* 9:47-58, 1981.
9. DENOTH, J. Load on the locomotor system and modelling. In: *Biomechanics of Running Shoes*, B. M. Nigg (Ed.). Champaign, IL: Human Kinetics Publishers, 1986, pp. 63-117.

10. FREDERICK, E. C., J. L. HAGY, and R. A. MANN. Prediction of vertical impact force during running (Abstract). *J. Biomech.* 14:498, 1981.
11. FREDERICK, E. C., T. E. CLARK, and C. L. HAMILL. Shoe design and rearfoot control in running (Abstract). *Med. Sci. Sports* 15:171, 1983.
12. HLAVAC, H. F. *The Foot Book*. Mountain View, CA: Anderson World, Inc., 1977, pp. 88–96.
13. JAMES, S., B. BATES, and L. OSTERNIG. Injuries in runners. *Am. J. Sports Med.* 6:40–50, 1978.
14. KRAHL, H. Das elastomechanische Verhalten der Patellarsehne (the elasto mechanic properties of the patellar tendon). *Sportarzt u. Sportmedizin* 10:285–289, 1977.
15. NIGG, B. M. Biomechanics, load analysis and sport injuries in the lower extremities. *Sports Medicine* 2:367–279, 1985.
16. NIGG, B. M. Experimental techniques used in running shoe research. In: *Biomechanics of Running shoes*, B. M. Nigg (Ed.). Champaign, IL: Human Kinetics Publishers, 1986, pp. 27–61.
17. NIGG, B. M., G. EBERLE, D. FREY, B. SEGESSER, and B. WEBER. Bewegungsanalyse fuer Schuhkorrekturen (Movement analysis for shoe corrections). *Medita* 9a:160–163, 1977.
18. NIGG, B. M. and S. M. LUETHI. Bewegungsanalysen beim Laufschuh (Movement analysis for running shoes). *Sportwissenschaft* 3:309–320, 1980.
19. NIGG, B. M., A. H. BAHLESEN, J. DENOTH, S. M. LUETHI, and A. STACOFF. Factors influencing kinetic and kinematic variables in running. In: *Biomechanics of Running Shoes*, B. M. Nigg (Ed.). Champaign, IL: Human Kinetics Publishers, 1986, pp. 139–159.
20. RADIN, E. L., R. B. ORR, and J. L. KELMAN, I. L. PAUL, and R. M. ROSE. Effect of prolonged walking on concrete on the knees of sheep. *J. Biomech.* 15:487–492, 1982.
21. SCHUSTER, R. O. *Biomechanical Running Problems*. Sports Medicine '78. NY: Futura Publishing Co., 1978, pp. 43–54.
22. SEGESSER, B. and B. M. NIGG. Insertionstendinosen am Schienbein, Achillodynie und Ueberlastungsfolgen am Fuss—Aetiologie, Biomechanik, therapeutische Moeglichkeiten (Tibial insertion tendinosis, achillodynia and damage to overuse of the foot—Etiology, biomechanics, therapy). *Orthopaede* 9:207–214, 1980.
23. SEGESSER, B., B. M. NIGG and F. MORELL. Achillodynie und tibiale Insertionstendinosen (Achillodynia and tibial insertion tendinosis). *Med. u. Sport* 20:79–83, 1980.
24. STACOFF, A. and X. KÄELIN. Pronation and sportshoe design. In: *Biomechanical Aspects of Sport Shoes and Playing Surfaces*, B. M. Nigg and B. A. Kerr (Eds.). Calgary, Canada: University Printing, 1983, pp. 143–151.
25. STACOFF, A. and S. LUETHI. Special aspects of shoe construction and foot anatomy. In: *Biomechanics of Running Shoes*, B. M. Nigg (Ed.). Champaign, IL: Human Kinetics Publishers, 1986, pp. 117–137.
26. STEINBRUECK, K. and H. CORTA. Epidemiologie und Sportverletzungen (Epidemiology of injuries in sports). *Deutsche Z. f. Sportmedizin* 34:173–186, 1983.
27. SUBOTNICK, S. I. The flat foot. *Physician Sports Med.* 9:85–91, 1981.
28. VOLOSHIN, A. and J. WOSK. An *in vivo* study of low back pain and shock absorption in the human locomotor system. *J. Biochem.* 15:21–27, 1982.
29. YAMADA, H. *Strength of Biological Materials*. Baltimore, MD: Williams & Wilkins, 1970, pp. 19–104.

## APPENDIX 1

TABLE A1.1. Summary of mean and SE (in parentheses) for the variables of interest in the project.

| No. of subjects                  | N                    |       | 14              | 14              | 14               |
|----------------------------------|----------------------|-------|-----------------|-----------------|------------------|
| Contact time                     | T                    | ms    | 237.3<br>(4.0)  | 234.9<br>(4.0)  | 228.9<br>(3.3)   |
| Initial joint pronation          | $\Delta\beta_{10}$   | deg   | 8.1<br>(1.0)    | 6.7<br>(1.1)    | 4.9<br>(0.9)     |
| Initial shoe pronation           | $\Delta\gamma_{10}$  | deg   | 6.6<br>(0.8)    | 4.9<br>(0.8)    | 3.6*<br>(0.7)    |
| Initial joint pronation velocity | $\dot{\beta}_{10}$   | deg/s | 301.0<br>(39.5) | 255.4<br>(42.0) | 190.5*<br>(36.6) |
| Initial shoe pronation velocity  | $\dot{\gamma}_{10}$  | deg/s | 236.7<br>(28.7) | 177.9<br>(29.0) | 138.6*<br>(27.4) |
| Total joint pronation            | $\Delta\beta_{pro}$  | deg   | 15.1<br>(0.8)   | 15.1<br>(1.0)   | 14.1<br>(0.7)    |
| Total shoe pronation             | $\Delta\gamma_{pro}$ | deg   | 12.7<br>(0.6)   | 12.3<br>(0.8)   | 11.4<br>(0.8)    |
| Initial Achilles tendon angle    | $\beta_0$            | deg   | 176.8<br>(1.1)  | 176.2<br>(1.3)  | 179.4<br>(1.1)   |
| Initial rearfoot angle           | $\gamma_0$           | deg   | 101.7<br>(0.8)  | 101.8<br>(1.0)  | 98.7*<br>(0.7)   |
| Initial sole angle               | $\delta_0$           | deg   | 29.8<br>(1.4)   | 29.0<br>(1.4)   | 27.0<br>(1.3)    |
| Initial knee angle               | $\epsilon_0$         | deg   | 166.0<br>(2.3)  | 165.8<br>(1.7)  | 164.3<br>(1.9)   |
| Vertical touch-down velocity     | $v_{oz}$             | deg   | 0.90<br>(0.08)  | 1.03<br>(0.08)  | 1.06<br>(0.06)   |
| Vertical impact force peak       | $F_{z1}$             | N     | 1,328<br>(82)   | 1,289<br>(86)   | 1,326<br>(94)    |
| Occurrence of $F_{z1}$           | $t_{z1}$             | ms    | 37.6<br>(1.9)   | 34.1<br>(2.2)   | 29.1*<br>(1.1)   |
| Maximum vertical loading rate    | $G_{z1}$             | kN/s  | 70.6<br>(8.7)   | 69.3<br>(7.6)   | 82.7<br>(9.0)    |

\* Indicates a significant difference between shoe A and shoe C determined with a one-way analysis of variance with a multiple range test (Tukey-B procedure) and  $\alpha = 0.05$ .

## APPENDIX 2

Determination of the change in spring constant for heel/shoe combination due to change of sole angle:

Assumptions:

- 1) the shoe sole can be described as a sum of parallel springs
- 2) the heel stiffness is independent of the position of the foot
- 3) geometry is as illustrated in Figure A2.1
- 4)  $\gamma = 90^\circ$
- 5) the contact area A is a circle with  $A = \pi r^2$ .

Solution:

for parallel springs, the spring constant f can be written as:

$$f = f_1 + f_2 + \dots + f_n$$



where in our example

$$f_i = f_k$$

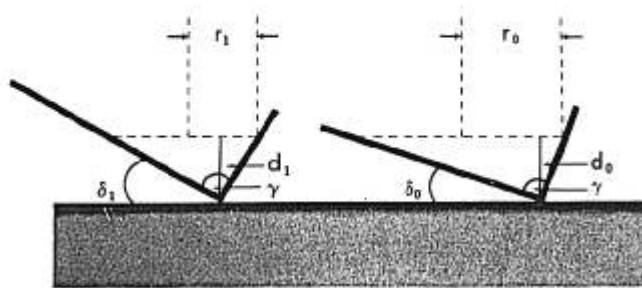


Figure A2.1—Illustration for the geometrical configuration and the assumptions for the estimation of the change in spring constant due to different sole position (two-dimensional). This model can be used for changes of sole and foot positions for the lateral or posterior view.

and therefore

$$f = n \cdot f_i$$

with  $n$  depending on the area

$$n = \text{number of spring elements}$$

$$n = (\text{total area}) : (\text{unit area})$$

the two spring constants depend on the area of contact

$$f_i : f_o = A_1 : A_o$$

$$f_i = f_o + \Delta f = f_o (A_1 : A_o)$$

determination of the area as a function of geometry:

$$A = \pi r^2$$

$$r = b : (2 \cdot \cos \delta)$$

$$b = d : \sin \delta$$

$$A = (\pi d^2) : (f \cdot \sin^2 \delta \cdot \cos^2 \delta)$$

$$(A_1 : A_o) = (d_1^2 \cdot \sin^2 \delta_o \cdot \cos^2 \delta_o) : (d_o^2 \cdot \sin^2 \delta_1 \cdot \cos^2 \delta_1)$$

for small changes of  $\delta$ , we assume that  $d_1 = d_o$ , therefore:

$$f_i = f_o \cdot (\sin^2 \delta_o \cdot \cos^2 \delta_o) : (\sin^2 \delta_1 \cdot \cos^2 \delta_1).$$